Rock and Soil Mechanics

Volume 43 | Issue 8 Article 2

9-30-2022

Progressive failure strength characteristics of anisotropic rocks caused by mineral directional arrangement: a case of biotite quartz schist

Han BAO
School of Highway, Chang'an University, Xi'an, Shaanxi 710064, China

Zhi-yang CHEN
School of Highway, Chang'an University, Xi'an, Shaanxi 710064, China

Heng-xing LAN
Institute of Geographic Sciences and Natural Resources Research, Chinese Academy of Sciences, Beijing 100101, China

Run-sheng PEI
School of Highway, Chang'an University, Xi'an, Shaanxi 710064, China

See next page for additional authors

Custom Citation

BAO Han, CHEN Zhi-yang, LAN Heng-xing, PEI Run-sheng, WU Fa-quan, YAN Chang-gen, TAO Yue, . Progressive failure strength characteristics of anisotropic rocks caused by mineral directional arrangement: a case of biotite quartz schist[J]. Rock and Soil Mechanics, 2022, 43(8): 2060-2070.

Progressive failure strength characteristics of anisotropic rocks caused by mineral directional arrangement: a case of biotite quartz schist

Authors

Han BAO, Zhi-yang CHEN, Heng-xing LAN, Run-sheng PEI, Fa-quan WU, Chang-gen YAN, and Yue TAO

Rock and Soil Mechanics 2022 43(8): 2060−2070 ISSN 1000−7598
https: //doi.org/10.16285/j.rsm.2021.6833 rocksoilmech.researchcommons.org/journal

Progressive failure strength characteristics of anisotropic rocks caused by mineral directional arrangement: a case of biotite quartz schist

BAO Han[1], CHEN Zhi-yang[1], LAN Heng-xing[2], PEI Run-sheng[1], WU Fa-quan[3], YAN Chang-gen[1], TAO Yue[1]

1. School of Highway, Chang'an University, Xi'an, Shaanxi 710064, China
2. Institute of Geographic Sciences and Natural Resources Research, Chinese Academy of Sciences, Beijing 100101, China
3. School of Civil Engineering, Shaoxing University, Shaoxing, Zhejiang 312000, China

Abstract: To explore the strength characteristics of anisotropic rocks caused by mineral directional arrangement during progressive failure process, biotite quartz schist was taken as an example, and triaxial compression tests were carried out on samples with schistosity angles of 0°, 45° and 90°. The macro and micro failure characteristics and progressive failure strength index of the specimens were analyzed, and the differences with other types of anisotropic rock were discussed. The results show that the failure characteristics of biotite quartz schist are closely related to its schistosity. With the schistosity angle increasing from 0° to 90°, the main macro and micro fracture modes of the specimens change from tensile to shear, and then to co-existence of tensile and shear. The strength characteristic values of biotite quartz schist show significant anisotropy. With the increase of schistosity angle, the strengthening effect caused by confining pressure increase on the strength characteristic values weakens, but the change of the strength value has a trend of acceleration. The anisotropic variation law of the ratio of strength characteristic value is not obvious, which gradually weakens and even disappears under high confining pressure. The fracture modes, variations of strength characteristic values and their ratios of anisotropic rocks with directional arrangement of minerals are different from those of rocks with stratified structure. A thorough understanding of the mechanical properties of rocks with directional arrangement of minerals will be helpful to guide the related engineering practice.

Keywords: mineral directional arrangement; biotite quartz schist; progressive failure; characteristic value of strength; anisotropy

1 Introduction

Rock failures are progressive mechanical behaviors, and many rock engineering problems are not only controlled by the influence of rock mass structure[1] but also closely related to the progressive failure process of rocks[2–4]. It is of great significance for roadway support[5], slope protection[6], and deep rock mass engineering construction[7] to clarify the progressive failure process of the rock and its mechanical evolution law, and to master the failure characteristics.

The progressive failure of rocks is actually the process of initiation, expansion, and coalescence of micro-cracks inside the rocks[8–9]. The development process of cracks inside the rock can be divided into different stages, and the stages are separated by four strength characteristic values, namely, compaction strength σ_{cc}, crack initiation strength σ_{ci}, damage strength σ_{cd}, and peak strength σ_f [10]. Among the four values of strength characteristic, σ_{cc} represents the closure of internal cracks in the rock, and σ_{ci} is the beginning mark of the stable crack propagation stage. σ_{cd} indicates the beginning of the reversal of the total volume strain and the unstable propagation of the crack[11], and the volume strain of the crack increases rapidly, the total volume strain begins to decrease, and the crack coalesces until the final failure at this stage[12]. Martin et al.[13–14] found that σ_{cc}/σ_f was mostly concentrated in 20%–40%, σ_{ci}/σ_f concentrated in 40%–60%, and σ_{cd}/σ_f concentrated in 70%–90%.

In recent years, studies on the progressive failure process of rocks have been carried out continuously. The rapid development of testing technology facilitates the accurate acquisition of rock failure characteristics. Both CT scanning and acoustic emission methods can be used to reveal the progressive failure process of rocks[15–17]. Theoretical and numerical methods, such as numerical manifold method[18], finite element method[19], and discrete element method[20], are mainly applied to the study of the mechanical mechanism of rock progressive failure. However, traditional research methods based on laboratory failure tests under mechanical loading and precise observation of fracture sections[10, 14, 21] cannot reflect the real-time fracture process, but they are convenient to carry out quantitative analysis of the progressive failure process of rocks from the perspective of mechanical characteristic values. Therefore, the traditional research method is still one of the most important means to study the

Received: 1 November 2021 Revised: 24 January 2022
This work was supported by the National Natural Science Foundation of China (42177142, 41927806, 42041006), the Youth Talent Promotion Program of Xi'an Association for Science and Technology (095920201310), and the Fundamental Research Funds for the Central Universities, Chang'an University (300102212213).
First author: BAO Han, male, born in 1988, PhD, Professor, mainly engaged in teaching and research work in geotechnical engineering and geological engineering. E-mail: baohangeo@163.com
Corresponding author: WU Fa-quan, male, born in 1955, PhD, Research scientist，PhD supervisor, research interests: theory and application of engineering geology and rock mechanics. E-mail: wufaquan@mail.igcas.ac.cn

progressive failure of rocks.

With the increasing research on the strength characteristic values and progressive failure of rocks, a deep understanding of their influencing factors and performance characteristics has also been obtained. Studies have found that the characteristic value of strength is affected by many factors such as confining pressure[22], size[23], and meso-and micro-structure[24–25] of the rock. The meso-and micro-structure and confining pressure of rock make its failure morphology and failure mechanical behavior show significant anisotropy and confining pressure effect[26], and the micro-structure determines the morphology characteristics of rock fracture[27] and the crack type is closely related to the confining pressure level[28].

At present, studies on the progressive failure of anisotropic rocks mostly focus on rocks with the anisotropy induced by layered structures, such as slate[29], shale[30], layered sandstone[17], and phyllite[31]. Relevant studies have also been carried out on the progressive failure of anisotropic rocks caused by the orientation of micro-fractures[32–33]. However, there are few studies on the characteristics of progressive failure strength of anisotropic rocks such as schist caused by the orientation of minerals[34]. In fact, there are differences in the failure phenomena of anisotropic rocks caused by mineral orientation and by layered structures. We take the shale with macroscopic layered structure as an example, when the angle between the loading direction and the bedding is small, the fracture mainly occurs along the relatively flat bedding plane, and the fracture plane bends obviously accompanied by the cracking of part of the bedding plane when the angle is large[35]. For the anisotropy of rocks caused by mineral orientation, the failure surfaces are rough and there are more bending sections, accompanied by more powders and debris[33]. The different failure patterns of different types of rocks are the external manifestation of their progressive failure process. Therefore, the mechanical characteristics of anisotropic rocks caused by mineral orientation in the progressive failure process need to be further explored.

Biotite quartz schist is a typical mineral-oriented rock with strong anisotropy[36]. In this paper, the biotite quartz schist was selected as the research object, the characteristic values of strength and shear strength parameters of specimens with different schistose plane directions were discussed, and the failure modes of biotite quartz schist were analyzed based on the triaxial compression test. The macro and micro failure characteristics and progressive failure mechanics characteristics of biotite quartz schist were revealed, and the influences of confining pressure and schistosity plane angle were accordingly analyzed. The research results will be helpful to guide the development of mineral-induced anisotropic rock engineering.

2 Materials and methods

The biotite quartz schist used in the experiment was taken from Xinjiang, China. The rock is hard and brittle, mainly composed of quartz, biotite, plagioclase, and a small number of other minerals. The minerals are oriented and form the schist structure (Fig. 1), which makes the rock exhibit significant anisotropy.

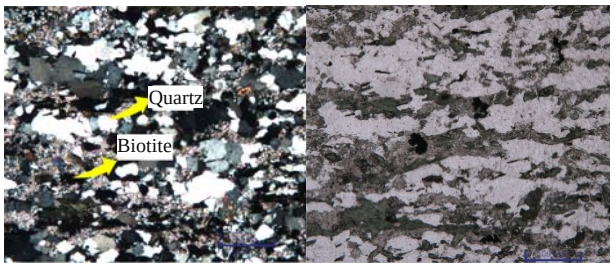

(a) 5×orthogonal image (b) 5×polarized image

Fig. 1 Microscopic characteristics of biotite quartz schist

In order to study the progressive failure strength characteristics of biotite quartz schist, the triaxial loading test was carried out on the specimen using the high-pressure rock triaxial dynamic test system (RTR-2000) produced by GCTS (Fig.2(a)). The tests were conducted at the Institute of Acoustics, Chinese Academy of Sciences. θ was defined as the angle between the biotite quartz schist schistosity plane and the loading direction (Fig. 2 (b)), and the cores were taken according to the angles $\theta = 0°$, 45°, and 90° respectively, and were processed into cylindrical rock specimens with a diameter of 25 mm and a height–diameter ratio of 2:1 (Figs. 2(c)–2(e)). The specimens were divided into three groups according to the angle θ, with four specimens in each group, and the average longitudinal wave velocity $\overline{V}_{\mathrm{p}}$ of each group was measured. The specimens with $\theta = 0°$ belong to the first

(a) High-pressure rock triaxial dynamic test system (b) The definition of angle θ

(c) θ=0° (d) θ=45° (e) θ=90°

Fig. 2 Mechanical test system and rock specimens

group, and $\overline{V}_{\mathrm{p}}=5\ 042.03$ m/ s. The specimens with $\theta=45°$ belong to the second group, and $\overline{V}_{\mathrm{p}}=4\ 680.47$ m/s. The specimens with $\theta=90°$ belong to the third group, and $\overline{V}_{\mathrm{p}}=3\ 882.36$ m/s. The wave velocities show great differences with the variation of θ, which reflects the significant anisotropy of biotite quartz schist. During the test, four confining pressures of 10, 20 , 30 , and 50 MPa were set for each group of specimens, and the axial loading rate was 0.03 mm/min.

3 Strength and failure characteristics

3.1 Stress–strain curves and strength parameters

Under different confining pressures, the pre-peak stress–strain curves of all groups of specimens under loading are shown in Fig. 3. Obviously, the peak strength of rock gradually increases with the increase of confining pressure, and generally decreases first and then increases with the increase of angle θ.

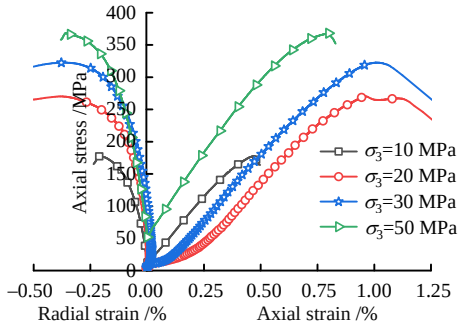

(a) θ=0° specimen

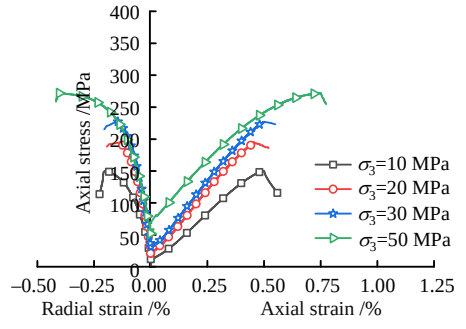

(b) θ=45° specimen

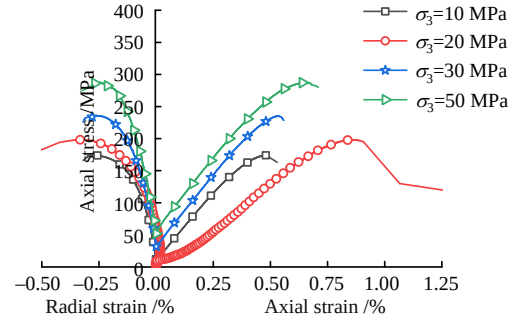

(c) θ=90° specimen

Fig. 3 Stress–strain curves of three groups of biotite quartz schist specimens

The strength envelope (Fig. 4) of the rock can be obtained from Fig.3, and the shear strength parameters of biotite quartz schist with three schistosity plane angles (Table 1) are obtained based on the Mohr-Coulomb strength theory. It is found that the cohesion c is the smallest when θ=0° and the value of c increases gradually as θ increases, while the internal friction angle φ shows a trend of first decrease and then increase with the increase of θ. The changes of c and φ are mainly related to the mechanical action of the schistosity plane. When θ=0° , the tensile fracture is easy to occur between schistosity planes, so the cohesion force is small and the internal friction angle is large. When θ=45° , the shear–slip failure along the schistosity plane is easy to occur, which reduces the apparent value of internal friction angle and raises the apparent value of cohesion. When θ=90° , the effect of the schistosity plane is weakened, and the cohesion and internal friction angle of rock are enhanced. Those results are similar to the study of Liu et al.[37].

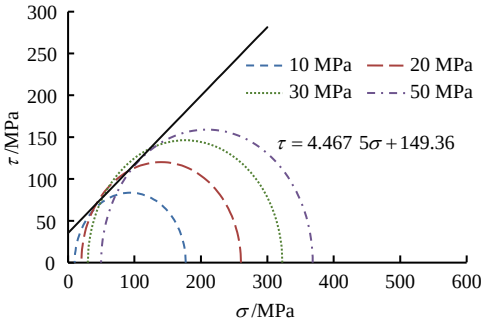

(a) θ=0°

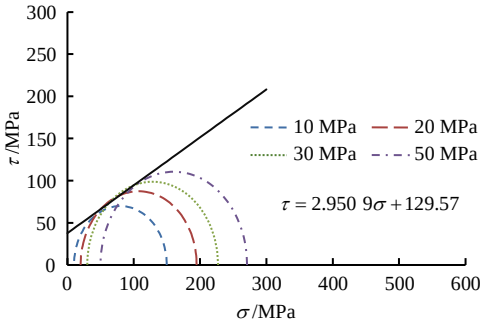

(b) θ=45°

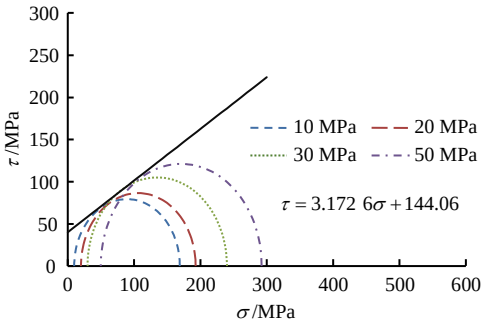

(c) θ=90°

Fig. 4 Strength envelope of rock specimens

Table 1 Shear strength parameters of biotite quartz schist

θ /(°)	Cohesion /MPa	Internal friction angle /(°)
0	35.3	39.4
45	37.7	29.6
90	40.0	31.5

3.2 Macro and micro characteristics of rock fracture surface

In fact, the confining pressure and schistosity plane have a great influence on the macro and micro characteristics of rock fracture surfaces[28, 38]. Figures 5 and 6 show the multi-scale fracture characteristics of all groups of specimens under different confining pressures.

The schistosity plane formed by the orientation of minerals has poor connectivity, so the main fracture surface of the biotite quartz schist is rough, and there are bends, more rock powder, and more rock debris (see Fig. 5). From Fig. 5, it can be observed that the failure surface of the specimen with θ=0° is rough, and the fracture mostly presents stepped, with a certain amount of rock powder. The fracture surface of the specimen with θ=45° is relatively straight, with a small amount of rock powder. The fracture surface of the specimen with θ=90° is rough and complex, and there is a large amount of rock powder. When the confining pressure increases from 10 MPa to 50 MPa, the straightness of the fracture surface and the amount of rock powder of each group of specimens increase correspondingly, and sliding scratches can be formed.

Figure 6 shows the SEM scanning results of the fracture micro-structure of all groups of specimens under confining pressure of 10 MPa and 50 MPa. In the figure, there are a large number of tensile fractures on the fracture surface of the specimen with θ=0° microscopically, and the micro-fracture surface presents a step-like feature, with a certain amount of rock powder. The micro-cracks on the fracture surface of the specimen with θ=45° mostly cut through the crystal, showing shear characteristics, and the micro fracture surface is relatively straight, with a small amount of rock powder. The fracture surface of the specimen with θ=90° shows the coexistence of tensile and shear fractures, and the fracture surface is rough and complex, with a large amount of rock powder. When the angle θ increases from 0° to 90°, the fracture of the specimen gradually shows a change from tensile fracture to shear fracture, then to the coexistence of tensile and shear fractures. With the increase of confining pressure, the microscopic fracture characteristics do not change much but the tensile fracture is restrained, the straightness of the fracture increases, and the rock powder increases accordingly.

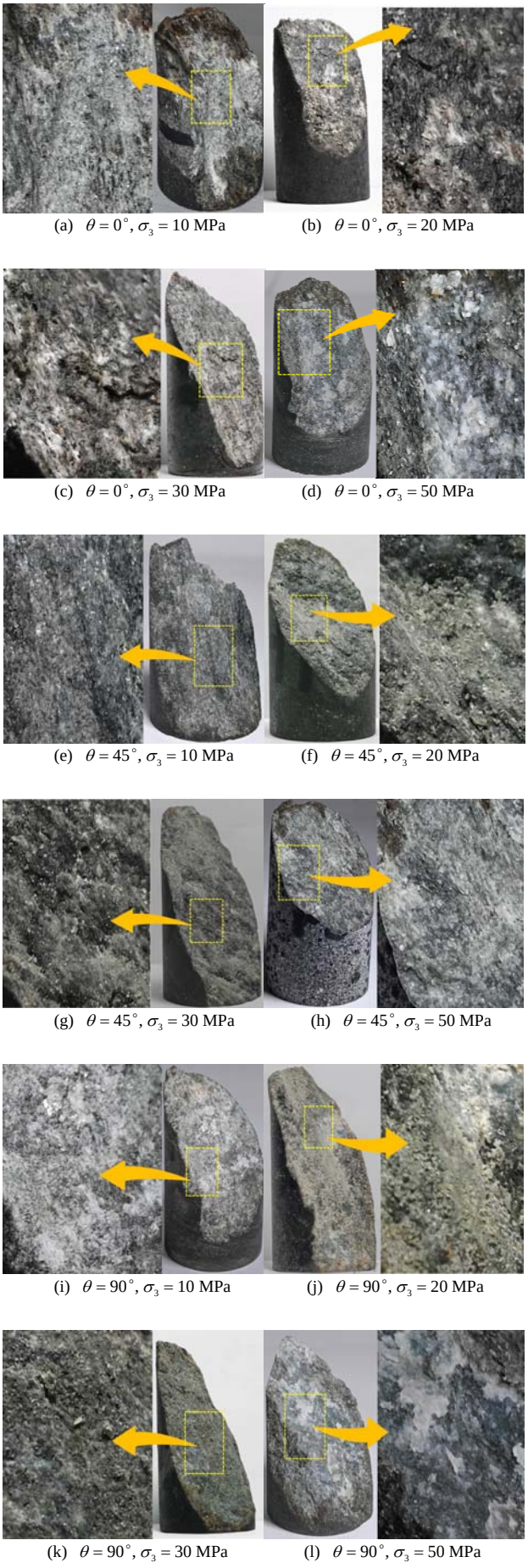

(a) $\theta = 0^\circ$, $\sigma_3 = 10$ MPa (b) $\theta = 0^\circ$, $\sigma_3 = 20$ MPa

(c) $\theta = 0^\circ$, $\sigma_3 = 30$ MPa (d) $\theta = 0^\circ$, $\sigma_3 = 50$ MPa

(e) $\theta = 45^\circ$, $\sigma_3 = 10$ MPa (f) $\theta = 45^\circ$, $\sigma_3 = 20$ MPa

(g) $\theta = 45^\circ$, $\sigma_3 = 30$ MPa (h) $\theta = 45^\circ$, $\sigma_3 = 50$ MPa

(i) $\theta = 90^\circ$, $\sigma_3 = 10$ MPa (j) $\theta = 90^\circ$, $\sigma_3 = 20$ MPa

(k) $\theta = 90^\circ$, $\sigma_3 = 30$ MPa (l) $\theta = 90^\circ$, $\sigma_3 = 50$ MPa

Fig. 5 Macroscopic pictures of fracture of specimens with different schistosity angles

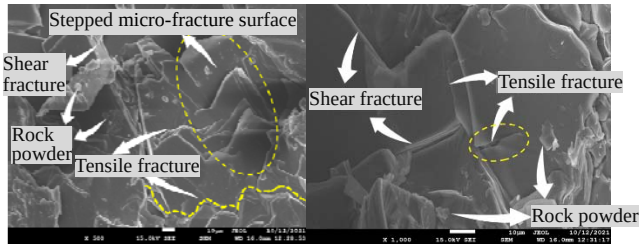

(a) $\theta = 0^\circ$, $\sigma_3 = 10$ MPa, 500× (b) $\theta = 0^\circ$, $\sigma_3 = 10$ MPa, 1 000×

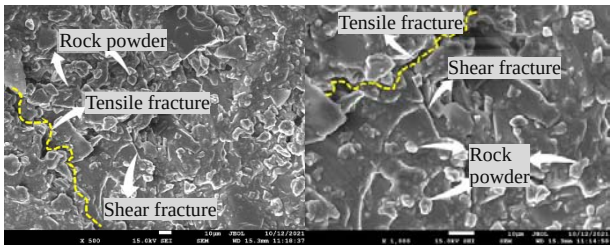

(c) $\theta = 0^\circ$, $\sigma_3 = 50$ MPa, 500× (d) $\theta = 0^\circ$, $\sigma_3 = 50$ MPa, 1 000×

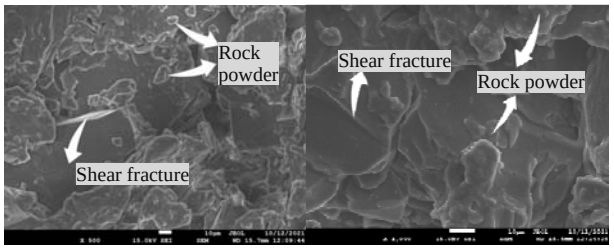

(e) $\theta = 45^\circ$, $\sigma_3 = 10$ MPa, 500× (f) $\theta = 45^\circ$, $\sigma_3 = 10$ MPa, 1 000×

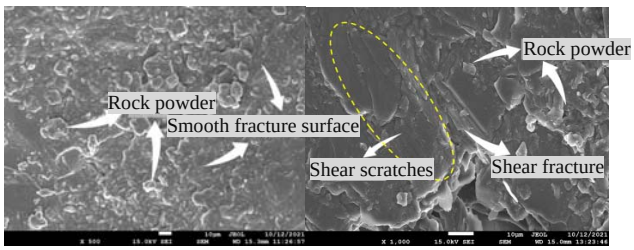

(g) $\theta = 45^\circ$, $\sigma_3 = 50$ MPa, 500× (h) $\theta = 45^\circ$, $\sigma_3 = 50$ MPa, 1 000×

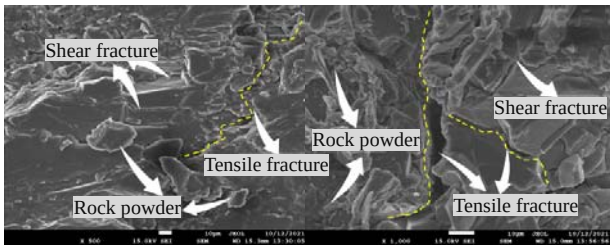

(i) $\theta = 90^\circ$, $\sigma_3 = 10$ MPa, 500× (j) $\theta = 90^\circ$, $\sigma_3 = 10$ MPa, 1 000×

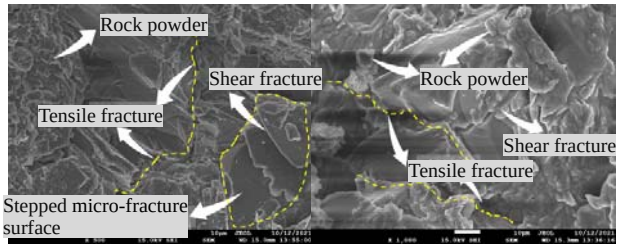

(k) $\theta = 90^\circ$, $\sigma_3 = 50$ MPa, 500× (l) $\theta = 90^\circ$, $\sigma_3 = 50$ MPa, 1 000×

Fig. 6 Microtopography of fracture of specimens with different schistosity angles

4 Progressive failure mechanical characteristics

4.1 Characteristic value of strength acquisition

The progressive failure process of the rock is actually the process of the continuous development of micro-cracks inside the rock. The progressive failure process can be quantitatively analyzed by characteristic values of strength such as σ_{cc}, σ_{ci}, σ_{cd}, and σ_f. Among the characteristic values of strength, σ_{cc} and σ_{ci} can be determined by the volumetric strain−axial strain curve of the crack, and σ_{cd} can be obtained by the total volumetric strain–axial strain curve, as shown in Fig. 7.

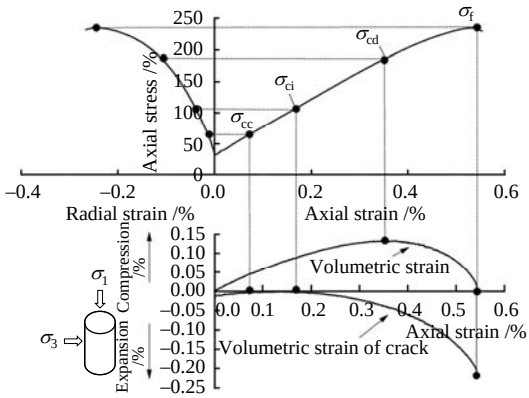

Fig.7 Stress–strain curves and strength characteristic point determination ((take the sample with 45° schistosity and 30 MPa confining pressure as an example)

The total volumetric strain ε_v and volumetric strain of the crack are respectively[13]

$$\varepsilon_v = \Delta V / V \approx \varepsilon_{axial} + 2\varepsilon_{lateral} \quad (1)$$

$$\varepsilon_{vc} = \varepsilon_v - \varepsilon_{ve} \quad (2)$$

where ε_{axial}, $\varepsilon_{lateral}$ are the axial and transverse strains, respectively; ε_{ve} is the elastic volumetric strain; $\varepsilon_{ve} = \dfrac{\Delta V}{V_{elastic}} = \dfrac{1-2v}{E(\sigma_1 - \sigma_3)}$, ΔV and $V_{elastic}$ are the specimen volume and elastic volume, respectively. The elastic modulus E and Poisson's ratio v are calculated from the linear elastic segment of the stress–strain curve.

4.2 Characteristic value of strength

According to table 2, the variation laws of characteristic values of strength of specimens with different schistosity angles under different confining pressure conditions are obtained, as shown in Figs. 8 and 9, and the performance rules of characteristic values of strength during the failure of biotite quartz schist are then obtained.

In Fig. 8, various characteristic values of strength for biotite quartz schist with different schistosity angles show a strengthening effect due to the increase

of confining pressure, but there are significant differences in the strengthening process. In this study, when the confining pressure increased from 10 MPa to 50 MPa, σ_f corresponding to θ=0°, 45°, and 90° increased by 107.6% (177.3–368.1 MPa), 80.9% (149.8–271.0 MPa), and 73.1% (168.9–292.3 MPa), respectively. σ_{cd} increased by 107.9% (150.3–312.5 MPa), 102.7% (115.3–233.7 MPa), and 89.0% (138.5–261.8 MPa). σ_{ci} increased by 122.0% (100.1–222.2 MPa), 143.4% (67.3–163.8 MPa), and 121.9% (80.3–178.2 MPa). σ_{cc} increased by 186.9% (45.1–129.4 MPa), 165.2% (37.0–98.3 MPa), and 167.4% (39.3–105.1 MPa), respectively. In general, the increase of the characteristic strength values follows compaction strength σ_{cc} > crack initiation strength σ_{ci} > damage strength σ_{cd} > peak strength σ_f . From the perspective of the curve shape, the strengthening effect of the characteristic strength values caused by the increase of the confining pressure tends to accelerate with the increase of the schistosity angle.

Table 2 Characteristic values of strength of biotite quartz schist

θ /(°)	Confining pressure /MPa	σ_{cc} /MPa	σ_{ci} /MPa	σ_{cd} /MPa	σ_f /MPa
0	10	45.1	100.1	150.3	177.3
	20	75.0	146.0	200.2	260.2
	30	108.0	196.5	266.2	322.5
	50	129.4	222.2	312.5	368.1
45	10	37.0	67.3	115.3	149.8
	20	51.8	85.2	174.4	194.9
	30	65.9	114.3	207.8	227.1
	50	98.3	163.8	233.7	271.0
90	10	39.3	80.3	138.5	168.9
	20	54.3	92.2	165.9	192.6
	30	67.7	116.4	205.9	240.1
	50	105.1	178.2	261.8	292.3

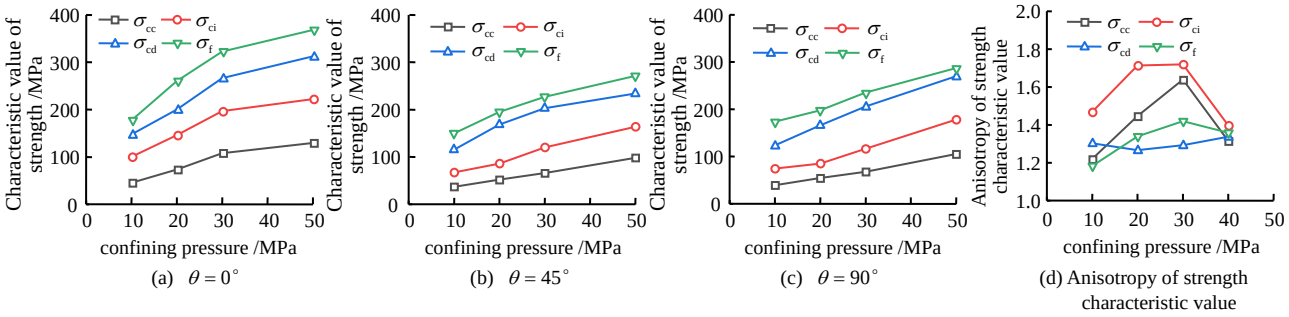

Fig. 8 Changes of characteristic strength values of specimens with different schistosity angles with the increase of confining pressure

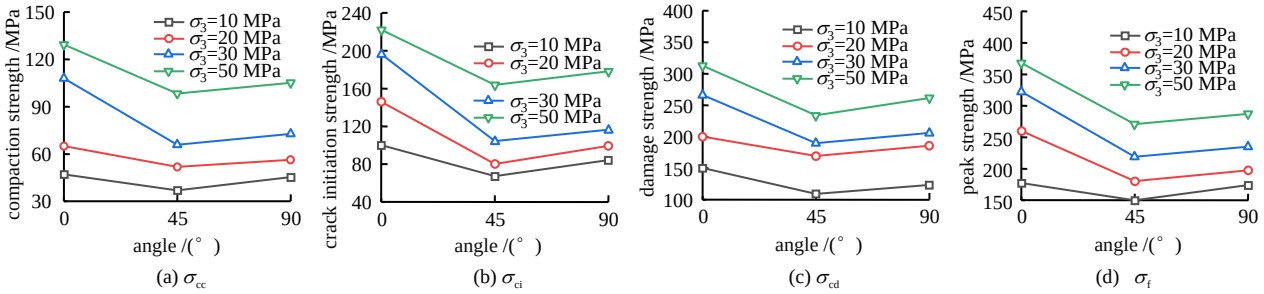

Fig. 9 Variation of strength characteristic values of specimens under different confining pressure with the schistosity angle

Studies have shown that the confining pressure can effectively inhibit the initiation and propagation of micro-cracks, especially the generation of tensile cracks[39-40], and this phenomenon is also reflected in this study. For example, when the schistosity angle is 0° , the strengthening effect induced by the confining pressure is the largest, the strengthening effect when the schistosity angle is 45° the second, and the strengthening effect when the schistosity angle is 90° is the weakest. It can be seen that the increase of confining pressure can inhibit the failure of the specimens with the schistosity angle of 0°, inside which more tensile fractures occur. In addition, according to Griffith theory[13], the initial fracture of rock is mainly the tensile fracture, so the inhibition of tensile fracture by the confining pressure is most obvious in the crack initiation strength. In this study, the strengthening effect induced by the increase of the confining pressure on the crack initiation strength is significantly larger than that on the peak strength and damage strength, which further confirms the inhibiting effect of the confining pressure on the tensile fracture.

The degree of anisotropy was defined in references[35, 40–41]. The ratio between the maximum and minimum values of characteristic values of strength in different directions was defined as the anisotropy coefficient of the characteristic value of strength. The influence of the confining pressure on the anisotropy coefficient of the characteristic value of strength is shown in Fig. 8(d). It can be seen that with the increase of the confining pressure, the anisotropy of the characteristic strength value of the anisotropic rock,

whose anisotropy is caused by the orientation of minerals, presents a trend of first increase and then decrease.

The variation of characteristic values of strength with the schistosity plane angle is shown in Fig. 9. When θ increases from 0° to 90°, the characteristic value of strength shows a typical U-shaped change. The mechanical effect produced by the schistosity plane with an angle 0° is similar to the "compression bar instability" between the schistosity planes, and the rock failure form is mainly splitting failure. The compressive strength of minerals is fully exerted, and the strength characteristic value of the rock is the largest. As a weak mechanical surface, the mechanical properties of the schistosity plane are exerted when the schistosity angle is 45°, which makes the specimen prone to shear failure along the schistosity plane. Therefore, the strength values of the specimen with the schistosity angle of 45° are small. For rocks with the schistosity angle of 90°, the shear failure of minerals between schistosity planes mainly occurs, and the strength of minerals is well exerted. In this case, the characteristic strength values of the rock are large.

4.3 Ratio of strength characteristic values

The ratio of strength characteristic values provides a basis for judging the failure stage of the rock. Figs. 10 and 11 show the variation of the ratio of strength characteristic values σ_{cc}/σ_f, σ_{ci}/σ_f, and σ_{cd}/σ_f with the confining pressure and schistosity plane angle during the loading process.

As illustrated by Figs. 10 (a) and 10 (c) that σ_{cc}/σ_f of each group of specimens increases with the increase of the confining pressure, from 0.25 when the confining pressure is 10 MPa to 0.35 when the confining pressure is 50 MPa, while σ_{ci}/σ_f shows a trend of first decrease and then increase with the increase of the confining pressure, and the changing trend of σ_{cd}/σ_f is not obvious. The ratio of the maximum value to the minimum value of the strength characteristic value ratio in different directions is defined as the anisotropy coefficient of characteristic strength value ratio. The influence of the confining pressure on the anisotropy coefficient of strength characteristic value ratio is shown in Fig. 10 (d). It can be seen that when the confining pressure reaches a certain degree, the anisotropy of the characteristic strength value ratio tends to disappear. In Fig. 8(d), the anisotropy changes of the four strength characteristic values show a similar development trend, and with the increase of the confining pressure, the anisotropy coefficients of the strength characteristic values show a convergence phenomenon. Therefore, the anisotropy coefficient of the strength characteristic value ratio in Fig. 10 (d) is lower than that in Fig. 8 (d). The anisotropy coefficient of the characteristic strength values is between 1.18 and 1.71, while the anisotropy coefficient of the strength characteristic value ratio is between 1.01 and 1.28.

It can be inferred that the anisotropy of the strength characteristic value is stronger than the anisotropy of the strength characteristic value ratio. In Fig. 11, the schistosity plane angle has no obvious regular effect on the ratio of strength characteristic values, indicating that for mineral-induced anisotropic rocks, the anisotropy of the strength characteristic value ratio is not strong, and the anisotropy is weakened or even disappears especially under the condition of high confining pressure.

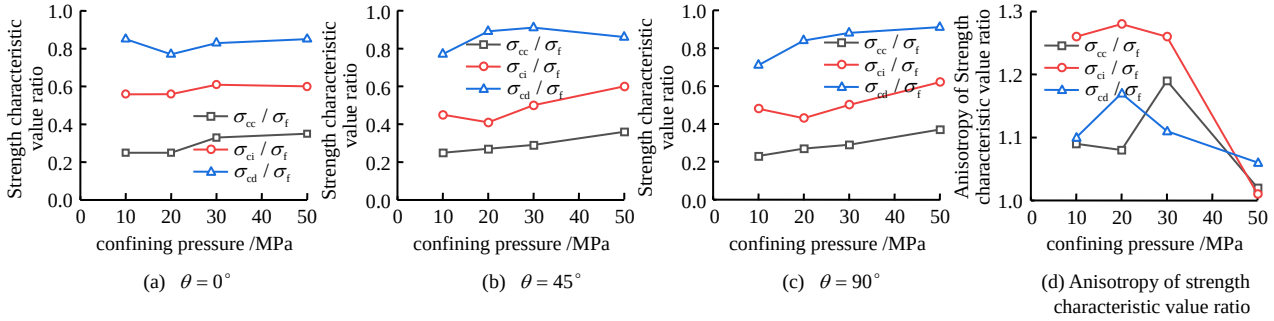

(a) $\theta = 0°$ (b) $\theta = 45°$ (c) $\theta = 90°$ (d) Anisotropy of strength characteristic value ratio

Fig. 10 Ratios of strength characteristic values vary with the confining pressure

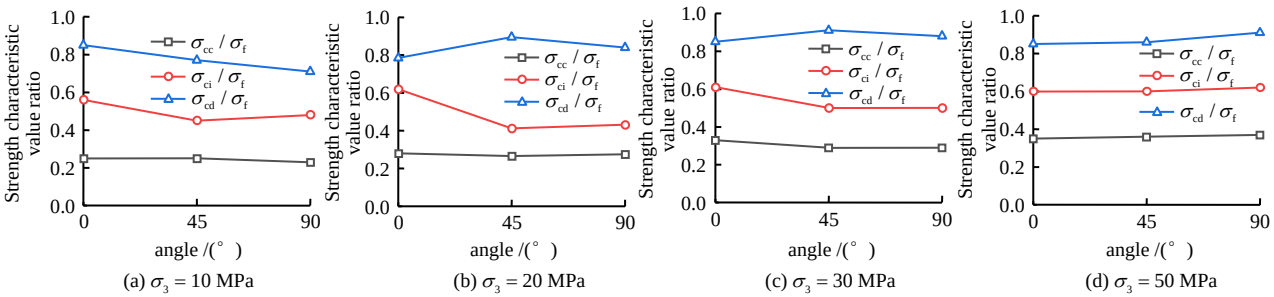

(a) σ_3 = 10 MPa (b) σ_3 = 20 MPa (c) σ_3 = 30 MPa (d) σ_3 = 50 MPa

Fig. 11 Ratios of characteristic strength values vary with the schistosity plane angle

5 Discussions

Biotite quartz schist is a typical mineral-induced anisotropic rock, and the oriented distribution of its minerals is an important feature that is different from other types of rocks. Based on the grayscale principle, the microscopic images of the specimens with the schistosity angle of 0°, 45°, and 90° are binarized by using the PCAS software[42] (the white areas are biotite minerals, and the black areas are quartz and other minerals (Figs. 12(a), 12(c), and 12(e)). The orientation of mineral particle arrangement is statistically analyzed, and the results are shown in Figs. 12(b), 12(d), and 12(f).

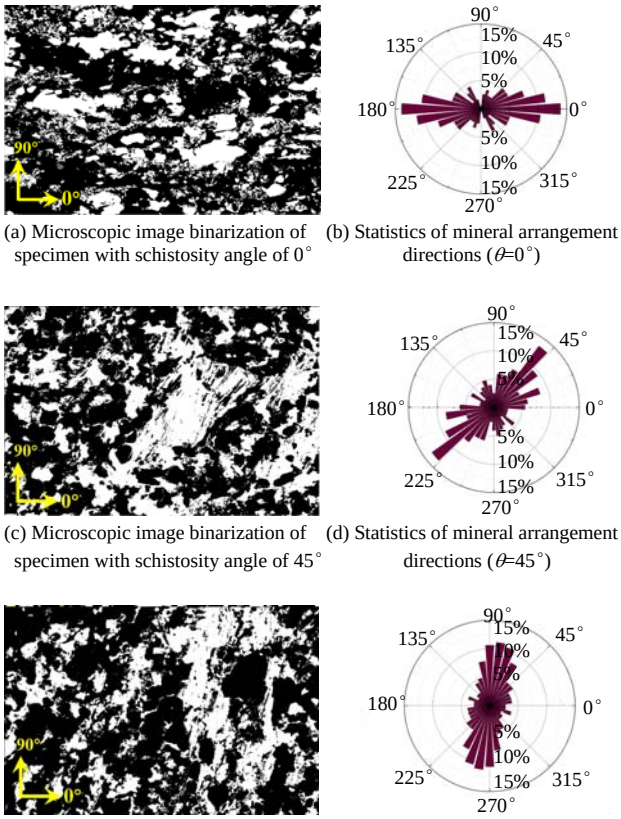

(a) Microscopic image binarization of specimen with schistosity angle of 0° (b) Statistics of mineral arrangement directions (θ=0°)

(c) Microscopic image binarization of specimen with schistosity angle of 45° (d) Statistics of mineral arrangement directions (θ=45°)

(e) Microscopic image binarization of specimen with schistosity angle of 90° (f) Statistics of mineral arrangement directions (θ=90°)

Fig. 12 Spatial characteristics of mineral orientation of biotite quartz schist

The orientation degree of minerals in the biotite quartz schist is relatively high, which makes the rock exhibit anisotropic characteristics. Due to the poor connectivity of the schistosity plane formed by the orientation of minerals, so the main fracture surface of the biotite quartz schist is rough and there are bends, more rock powder, and more rock debris. These characteristics are quite different from the failure of rocks containing macro bedding planes, such as shale[35], which often exhibit flat failure surfaces when the angle between the loading direction and the bedding plane is small, and curved fracture surfaces when the angle is large.

The results show that the strength of biotite quartz schist when the angle between the loading direction and the schistosity plane is 0° is greater than that when the angle is 90°, which is consistent with the performance characteristics of mica quartz schist, chlorite schist, and shale[33, 35–37]. At the same time, it is found that for biotite quartz schist, the strengthening effect induced by the increasing confining pressure on each strength characteristic value follows the schistosity plane angle order of 0° >45° >90°. However, for the initiation strength of bedding shale, the strengthening effect induced by the confining pressure is the weakest when the schistosity plane angle is 45°[43]. The anisotropy of the strength characteristic value of biotite quartz schist increases first and then decreases with the increase of confining pressure. However, the anisotropy degree of the strength characteristic value of bedding rocks gradually decreases with the increase of confining pressure[35, 39, 43].

The strength characteristic value ratios of biotite quartz schist σ_{ci}/σ_f = 0.44–0.61 and σ_{cd}/σ_f = 0.77–0.92. Studies on approximately homogeneous rocks and bedding rocks show that the values of σ_{ci}/σ_f and σ_{ci}/σ_f of approximately homogeneous rocks such as marble[44–45] and granite[14] are relatively small, showing σ_{ci}/σ_f = 0.40–0.47 and σ_{cd}/σ_f = 0.70–0.85. The variation range of strength characteristic value ratio of bedding rocks is slightly larger, such as σ_{ci}/σ_f = 0.43–0.81 and σ_{cd}/σ_f = 0.76–0.96 for shale[43].

The strength characteristic value ratio σ_{cd}/σ_f of biotite quartz schist does not change obviously with the increase of confining pressure, while σ_{ci}/σ_f decreases first and then increases. The strength characteristic value ratio σ_{cd}/σ_f of bedding shale increases first and then decreases with the increase of confining pressure, while σ_{ci}/σ_f increases continuously[43]. The ratio of strength characteristic value of homogeneous rocks decreases with the increase of confining pressure[45].

6 Conclusions

The progressive failure strength characteristics of anisotropic rocks caused by the orientation of minerals have certain particularities. Taking biotite quartz schist as an example, this paper studies the macro and micro failure morphology characteristics and progressive failure strength characteristics of anisotropic rocks caused by the orientation of minerals based on triaxial compression tests, and draws the following main conclusions:

(1) The failure morphology of anisotropic rocks caused by the orientation of minerals is closely related to their schistosity structure, and the main fracture plane is characterized by rough bending and more rock powder and debris. When the angle of schistosity plane increases from 0° to 90°, the rock fracture gradually shows a change from mainly tensile fracture to shear fracture, then to the coexistence of the tensile

and shear fractures. With the increase of confining pressure, the tensile fracture is restrained, the straightness of macro and micro fracture surfaces increases, and rock powder increases accordingly.

(2) The strength characteristic values of anisotropic rocks caused by the orientation of minerals during progressive failure process have significant anisotropy, and the strength characteristic values show a typical U-shaped change with the increase of the angle of schistosity plane. The strengthening effect induced by the confining pressure on the strength characteristic values varies with the angle of schistosity plane, which follows the order of 0°>45°>90°, but the strengthening effect of the strength characteristic value produced by the confining pressure tends to accelerate with the increase of the angle of schistosity plane.

(3) The strength characteristic value ratio σ_{cc}/σ_f of anisotropic rock caused by the orientation of minerals increases with increasing confining pressure, while σ_{ci}/σ_f first decreases and then increases with increasing confining pressure, but the change of σ_{cd}/σ_f is not obvious. The anisotropy of strength characteristic value ratio of mineral-induced anisotropic rocks is not obvious, and the anisotropy is weakened or even disappears under high confining pressure.

(4) The mechanical behavior of mineral-induced anisotropic rocks is affected by the orientation of minerals, and it is different from that of bedding rocks in terms of failure form, strength characteristic value, and strength characteristic value ratio, and the influence of the confining pressure is significantly different.

References

[1] BAO Han, XU Xun-hui, LAN Heng-xing, et al. Stiffness model of rock joint by considering anisotropic morphology[J]. Journal of Traffic and Transportation Engineering, 2022, 22(2): 160–175.

[2] JIANG Quan, FENG Xia-ting, LI Shao-jun, et al. Cracking-restraint design method for large underground caverns with hard rock under high geostress condition and its practical application[J]. Chinese Journal of Rock Mechanics and Engineering, 2019, 38(6): 1081–1101.

[3] KONG Chao, HOU Zhi-qiang, ZHU Xiao-yu, et al. Model test study on progressive failure law of soft surrounding rock in large section Metro station tunnel[J]. China Railway Science, 2020, 41(1): 78–84.

[4] DAI Feng, LI Biao, XU Nu-wen, et al. Characteristics of damaged zones due to excavation in deep underground powerhouse at Houziyan hydropower station[J]. Journal of Rock Mechanics and Engineering, 2015, 34(4): 735–746.

[5] BAI Q S, TU S H, ZHANG C, et al. Discrete element modeling of progressive failure in a wide coal roadway from water-rich roofs[J]. International Journal of Coal Geology, 2016, 167: 215–229.

[6] SONG Dan-qing, HUANG Jin, LIU Xiao-li, et al. Influence of the rock mass structure and lithology on the dynamic response characteristics of steep rock slopes during earthquakes[J]. Journal of Tsinghua University (Science and Technology), 2021, 61(8): 873880.

[7] NASSERI M H B, RAO K S, RAMAMURTHY T. Anisotropic strength and deformational behavior of Himalayan schists[J]. International Journal of Rock Mechanics and Mining Sciences, 2003, 40(1): 3–23.

[8] GUO S, QI S, ZHAN Z, BOWEN Z, et al. Plastic-strain-dependent strength model to simulate the cracking process of brittle rocks with an existing non-persistent joint[J]. Engineering Geology, 2017, 231: 114–125.

[9] LAN H X, MARTIN C D, HU B. Effect of heterogeneity of brittle rock on micromechanical extensile behavior during compression loading[J]. Journal of Geophysical Research, 2010, 115(B1): B01202.

[10] BAO Han, PEI Run-sheng, LAN Heng-xing, et al. Damage evolution of anisotropic rock caused by mineral directional arrangement under the cyclic loading and unloading test: a case of biotite quartz schist[J]. Chinese Journal of Rock Mechanics and Engineering, 2021, 40(10): 2015–2026.

[11] BIENIAWSKI Z T. Mechanism of brittle fracture of rock. Part I—theory of the fracture process[J]. International Journal of Rock Mechanics and Mining Sciences & Geomechanics Abstracts, 1967, 4(4): 395-404, IN11-IN12, 405–406.

[12] WEI L, LIU Q S, LIU X W. An improved crack initiation stress criterion for brittle rocks under confining stress[J]. IOP Conference Series: Earth and Environmental Science, 2018, 170(2): 022141.

[13] MARTIN C D, CHANDLER N A. The progressive fracture of Lac du Bonnet granite[J]. International Journal of Rock Mechanics and Mining Sciences & Geomechanics Abstracts, 1994, 31(6): 643–659.

[14] MARTIN C D, CHRISTIANSSON R. Estimating the potential for spalling around a deep nuclear waste repository in crystalline rock[J]. International Journal of Rock Mechanics and Mining Sciences, 2009, 46(2): 219–228.

[15] WANG Deng-ke, ZENG Fan-chao, WANG Jian-guo, et al. Dynamic evolution characteristics and fractal law of loaded coal fractures by micro industrial CT[J]. Chinese Journal of Rock Mechanics and Engineering, 2020, 39(6):

1165–1174.

[16] MA Tian-shou, WANG Hao-nan, LIU Meng-yun, et al. Experimental and theoretical investigation on anisotropy of shale tensile mechanical behaviors[J]. Journal of Central South University (Natural Science), 2020, 51(5): 1391–1401.

[17] CHU Chao-qun, WU Shun-chuan, ZHANG Shi-huai, et al. Mechanical behavior anisotropy and fracture characteristics of bedded sandstone[J]. Journal of Central South University (Natural Science), 2020, 51(8): 2232–2246.

[18] ZHANG Z, WANG S, WANG C, et al. A study on rock mass crack propagation and coalescence simulation based on improved numerical manifold method (NMM)[J]. Geomechanics and Geophysics for Geo-Energy and Geo-Resources, 2021, 7(1): 5.

[19] HE Y, YANG Z, LI X, et al. Numerical simulation study on three-dimensional fracture propagation of synchronous fracturing[J]. Energy Science and Engineering, 2020, 8(4): 944–958.

[20] YANG W M, GENG Y, ZHOU Z Q, et al. DEM numerical simulation study on fracture propagation of synchronous fracturing in a double fracture rock mass[J]. Geomechanics and Geophysics for Geo-Energy and Geo-Resources, 2020, 6: 39.

[21] PEI Run-sheng, BAO Han, LAN Heng-xing, et al. Evolution characteristics of elastic modulus and energy of biotite quartz schist under cyclic loading and unloading test[J/OL]. Journal of Engineering Geology , 1-13 [2022-07-07]. DOI: 10.13544/j.cnki.jeg.2022-0003.

[22] PENG Shuai, ZHANG Xi-wei, FENG Xia-ting, et al. Deformation behavior of Jinping marble under isotropic compression and deviatoric stress loading conditions[J]. Rock and Soil Mechanics, 2017, 38(12): 3532–3539, 3546.

[23] WU Fa-quan, QIAO Lei, GUAN Sheng-gong, et al. Uniaxial compression test study on size effect of small size rock samples[J]. Chinese Journal of Rock Mechanics and Engineering, 2021, 40(5): 865–873.

[24] YANG X J , WANG J M, ZHU C, et al. Effect of wetting and drying cycles on microstructure of rock based on SEM[J]. Environmental Earth Sciences, 2019, 78(6): 183.

[25] LAN Heng-xing, BAO Han, SUN Wei-feng, et al. Multi-scale heterogeneity of rock mass and its mechanical behavior[J]. Journal of Engineering Geology, 2022, 30(1): 37–52.

[26] CHEN Zi-quan, HE Chuan, WU Di, et al. Mechanical properties and energy damage evolution mechanism of deep-buried carbonaceous phyllite[J]. Rock and Soil Mechanics, 2018, 39(2): 445–456.

[27] TAO Ming, WANG Jun, LI Zhan-wen, et al. Meso-and micro-experimental research on the fracture of granite spallation under impact loads[J]. Chinese Journal of Rock Mechanics and Engineering, 2019, 38(11): 2172–2181.

[28] MU Kang, LI Tian-bin, YU Jin, et al. Mesoscopic simulation of relationship of acoustic emission and compressive deformation behaviour in sandstone under confining pressures effect[J]. Chinese Journal of Rock Mechanics and Engineering, 2014, 33(Suppl.1): 2786–2793.

[29] GHOLAMI R, RASOULI V. Mechanical and elastic properties of transversely isotropic slate[J]. Rock Mechanics and Rock Engineering, 2014, 47(5): 1763–1773.

[30] WANG Hong-jian, LIU Da-an, HUANG Zhi-quan, et al. Mechanical properties and brittleness evaluation of layered shale rock[J]. Journal of Engineering Geology, 2017, 25(6): 1414–1423.

[31] WU Yong-sheng, TAN Zhong-sheng, YU Yu, et al. Anisotropically mechanical characteristics of Maoxian group phyllite in northwest of Sichuan province[J]. Rock and Soil Mechanics, 2018, 39(1): 207–215.

[32] MA Ai-yang, WU Fa-quan, QI Sheng-wen, et al. Characteristics of unloading micro cracks in shallow rock mass at left bank of Jinping Ⅰ hydropower station dam[J]. Journal of Engineering Geology, 2017, 25(5): 1381–1388.

[33] YIN Xiao-meng, YAN E-chuan, HUANG Shao-ping, et al. Influence of microscopic characteristics on the anisotropy of crack initiation stress and crack propagation of schist[J]. Chinese Journal of Rock Mechanics and Engineering, 2019, 38(7): 1373–1384.

[34] ZHANG Xiao-ping, WANG Si-jing, HAN Geng-you, et al. Crack propagation study of rock based on uniaxial compressive test—a case study of schistose rock[J]. Chinese Journal of Rock Mechanics and Engineering, 2011, 30(9): 1772–1781.

[35] HENG Shuai, YANG Chun-he, ZHANG Bao-ping, et al. Experimental research on anisotropic properties of shale[J]. Rock and Soil Mechanics, 2015, 36(3): 609–616.

[36] WU Fu-bao. Experimental study on mechanical characteristics of mica quartz schist foliation surface[J]. Journal of Geotechnical Engineering, 2019, 41(Suppl.1): 117–120.

[37] LIU Sheng-li, CHEN Shan-xiong, YU Fei, et al. Anisotropic properties study of chlorite schist[J]. Rock and Soil Mechanics, 2012, 33(12): 3616–3623.

[38] LIU X, FENG X T, ZHOU Y. Experimental study of mechanical behavior of gneiss considering the orientation of schistosity under true triaxial compression[J]. International Journal of Geomechanics, 2020, 20(11): 04020199.

[39] CHEN Tian-yu, FENG Xia-ting, ZHANG Xi-wei, et al. Experimental study on mechanical and anisotropic properties of black shale [J]. Chinese Journal of Rock Mechanics and Engineering, 2014, 33(9): 1772–1779.

[40] HE Bai, XIE Ling-zhi, LI Feng-xia, et al. Anisotropic mechanism and characteristics of deformation and failure of Longmaxi shale(in Chinese)[J]. Scientia Sinica Physica, Mechanica & Astronomica, 2017, 47(11): 107–118.

[41] NIANDOU H, SHAO J F, HENRY J P, et al. Laboratory investigation of the mechanical behaviour of Tournemire shale[J]. International Journal of Rock Mechanics and Mining Sciences, 1997, 34(1): 3–16.

[42] YAN Gao-yuan, WEI Zhong-tao, SONG Yu, et al. Quantitative characterization of shale pore structure based on Ar-SEM and PCAS[J]. Earth Science, 2018, 43(5): 1602–1610.

[43] LI C B, XIE H P, WANG J. Anisotropic characteristics of crack initiation and crack damage thresholds for shale[J]. International Journal of Rock Mechanics and Mining Sciences, 2020, 126: 104178.

[44] FONSEKA G M, MURRELL S A F, BARNES P. Scanning electron microscope and acoustic emission studies of crack development in rocks[J]. International Journal of Rock Mechanics and Mining Sciences & Geomechanics Abstracts, 1985, 22(5): 273–289.

[45] LIU Ning, ZHANG Chun-sheng, CHU Wei-jiang. Fracture characteristics and damage evolution law of Jinping deep marble[J]. Chinese Journal of Rock Mechanics and Engineering, 2012, 31(8): 1606–1613.